

# Morphology–Property Relationships in Oriented Pet Films: A Role of In-Plane Crystalline Orientation Distribution on the Film Properties

RAMESH M. GOHIL

Du Pont, Circleville Research Laboratory, Circleville, Ohio 43113

## SYNOPSIS

The role of in-plane crystalline, amorphous, and overall molecular orientation on various properties in the plane of the films was investigated using a variety of techniques. It is shown that for a fixed value of crystallinity the in-plane crystalline orientation and the nature of the constraint imposed by the crystallites on the molecules play an important role in obtaining isotropic in-plane expansion or shrinkage properties. Achievement of in-plane isotropic tensile strength and elongation at the break are found to depend entirely upon an isotropic distribution of the amorphous orientation; the orientation of crystallites plays no detectable role. Furthermore, the deformation mechanisms of sequential and simultaneous biaxial stretching processes have been investigated and compared. The simultaneous stretching process is considered to be a more controlled film-fabricating method compared to sequential stretching in achieving balanced, in-plane film properties. © 1993 John Wiley & Sons, Inc.

## INTRODUCTION

This paper forms a part of our series of publications on morphology–property relationships in biaxially oriented PET films prepared by sequential and simultaneous stretching processes. The first paper in this series dealt with the development of orientation in the amorphous phase<sup>1</sup> and, the second, with changes in the crystalline structure during biaxial stretching.<sup>2</sup> Studies on the development of constraint on the amorphous molecules and its effect on properties such as the permeability of gases is carried out in a third publication,<sup>3,4</sup> whereas the present communication deals with criteria for preparing films having in-plane isotropic shrinkage or expansion. Many practical applications require excellent in-plane dimensional stability.

The microstructures produced by the simultaneous and sequential stretching processes have been extensively studied in the past<sup>5–10</sup> and were discussed

in the previous publications.<sup>1–4</sup> The present study deals with the effect of processing conditions on the structure of the film and, thereby, properties.

In the film of semicrystalline-oriented polymers, the nature of the amorphous phase plays an important role in controlling several properties like shrinkage, expansion, dye diffusion, gas permeability, and hydrolytic stability. For a particular degree of molecular orientation and molecular weight, the nature of the amorphous phase is modified by constraint on amorphous molecules by the nature of crystallites, their volume fraction, and proximity of the crystallites to the amorphous molecules. For several film applications, it is necessary to control the in-plane properties; however, the underlying mechanism to achieve this is not well understood. In this communication, it is our intent to demonstrate the role of distribution of the crystallites on the film properties with particular emphasis on achieving isotropic in-plane shrinkage or expansion of PET film. In addition, it is also our intent to shed some light on the deformation mechanisms involved in sequential and simultaneous stretching processes.

## EXPERIMENTAL

### Sample Preparation

The uniaxial, biaxial sequential, and biaxial simultaneous stretching processes have been defined previously.<sup>3</sup> The stretching operations were conducted at 90°C on a T. M. Long stretcher having a 4 × 4-in. pantograph capable of stretching up to 4.0× in both directions. In the sequential stretching process, the amorphous cast film is first stretched along a direction defined as the machine direction (MD) with a transverse direction (TD) restraint up to a draw ratio of 3.5×. Uniaxial stretching is carried out using amorphous cast film with constant width to a desired draw ratio at 90°C with a strain rate of 1.5 s<sup>-1</sup>. After completion of uniaxial stretching, in the second step, the film is stretched in the TD to a desired draw ratio (Fig. 1). Four different TD draw

ratios (1.0×, 1.5×, 2.25×, and 3.5×) are used for preparing sequentially, biaxially oriented films. In the simultaneous stretching process, MD× and TD× are varied at the same time to the desired level. Once the simultaneous process is started, deformation continues without interruption at a selected temperature. Subsequently, films are heat-set at 200°C for 5 min with fixed dimensions. Additive-free PET having a molecular weight of 20,000 is utilized for the study. The diethylene glycol content (DEG) in the present PET sample is 1.5 mol %.

### Sample Characterization

#### Electron Microscopy

Morphology of the films was directly observed in the transmission electron microscope on microtomed samples. Detailed information regarding

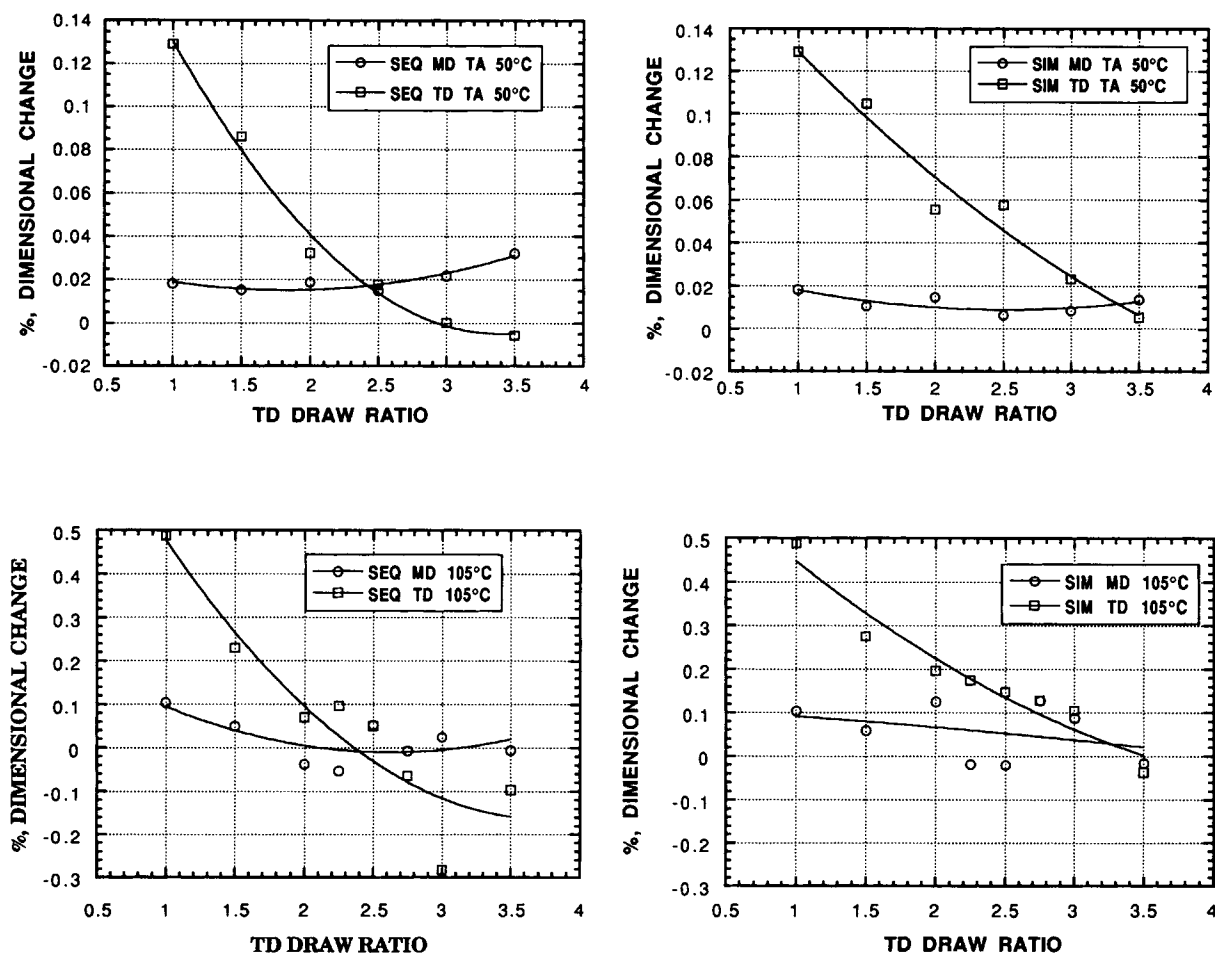


**Figure 1** Variation in dimensional changes at 50 and 105°C along the MD and TD with the TD stretch ratio in sequentially (SEQ) and simultaneously (SIM) stretched films.  $T_a$ , MD, and TD, respectively, represent annealing temperature, machine, and transverse directions.

sample preparation and defocused electron microscopy has been discussed previously.<sup>2</sup>

### X-Ray

The pole figures were obtained with a Picker "single-crystal" goniometer with Eulerian geometry and three axes (phi, chi, and two-theta) automated. Ni-filtered copper radiation was used as the X-ray source. Data obtained were processed by a Hewlett-Packard computer. A specimen is mounted in the instrument and aligned so that the MD is coincident with the direction  $\chi = 90$  (the north pole-south pole axis) and the surface normal (SN) or "thickness direction" (ThD) is directed along  $\phi = 0, \chi = 0$ ; the TD is then along  $\phi = 90, \chi = 0$ . The value for the pole figure for any phi-chi pair is determined by measuring the intensity at the two-theta value corresponding to the desired *hkl* reflection. Details regarding sample preparation, definitions of various directions, and angles have been discussed previously.<sup>3</sup>

The major information regarding the crystalline orientation can be obtained from the pole figure analysis of the (100) and ( $\bar{1}05$ ) planes. The ( $\bar{1}05$ ) reflection is the most suitable for monitoring *c*-axis orientation. In uniaxially oriented films, the *c*-axis (molecular direction) is mainly along the MD direction (along the north-south direction). In such a case, one observes intensity from the ( $\bar{1}05$ ) planes at the center of the pole figure. The spread in intensity indicates a deviation of the *c*-axis from the plane of the film. If crystals are oriented along both directions, MD and TD, then one observes a bimodal distribution in the intensity. Film having isotropic crystal orientation in the film plane will show a continuous band of uniform intensity at the center of the pole figure.<sup>3</sup> Wide- and small-angle X-ray scattering (WAXS and SAXS) experiments were conducted in the transmission mode, using  $\text{CuK}\alpha$  radiation and a flat-film camera. Single sheets of PET films (approximately 1 mm thick) were used for the SAXS exposures.

### Intrinsic Fluorescence

Recently it has been reported<sup>1</sup> that associated ground-state dimers of PET, consisting of two terephthalic moieties in the amorphous phase, can be used as a chain-intrinsic fluorescent label that reveals the amorphous orientation. This technique gives the average orientation of chains in the amorphous phase. PET dimers are excited at a wavelength,  $\lambda = 340$  nm, and, with the polarizer and an analyzer parallel, the specimen was rotated. The in-

tensity of fluorescence emission (at  $\lambda = 390$  nm) from the amorphous phase was measured every  $10^\circ$  of specimen rotation, and polar plots of in-plane angular distribution of polarized fluorescence emission intensity were obtained.

To achieve quantitative analysis of the proportion of noncrystalline chains oriented along the MD and TD, an "orientation ratio," *R*, was calculated as follows:

$$R_{\text{MD}} = \frac{I_{\text{MD}}}{I_{\text{MD}} + I_{\text{TD}}} \quad (1)$$

and

$$R_{\text{TD}} = \frac{R_{\text{TD}}}{I_{\text{MD}} + I_{\text{TD}}} \quad (2)$$

where  $I_{\text{MD}}$  and  $I_{\text{TD}}$  are the emission intensities obtained along machine and transverse draw directions of the film parallel to the polarization direction.

### Density Measurements

The densities of the PET films were obtained using a gradient density column made from toluene and carbon tetrachloride. The percentage crystallinity of the films were computed from

$$X = \frac{\rho_c (\rho - \rho_a)}{\rho (\rho_c - \rho_a)} \times 100 \quad (3)$$

where  $\rho$  is the density. The subscripts "c" and "a" denote the crystalline and amorphous phases, respectively. The density of the crystalline is taken as 1.455 g/cc and the amorphous phase is 1.333.<sup>11</sup>

### Refractive Index

Refractive indices of the films were carried out using an Abbe refractometer (Reichert-Jung). It provides information regarding molecular orientation from the crystalline and amorphous phases.<sup>12</sup>

### Thermal Mechanical Analyzer

Dimensional changes in the film were measured as a function of temperature by a DuPont 2940 thermal mechanical analyzer (TMA). The heating rate during TMA scan was  $20^\circ\text{C}/\text{min}$  and the force applied to the sample was 0.05 N.

### Mechanical Properties

The mechanical measurements were carried out on the film samples ( $2.5 \times 5.0$  cm) with a Model 1122

Instron machine at room temperature using a strain rate of 100%/min.

## RESULTS AND DISCUSSION

To understand how the distribution of crystalline and amorphous phases influence film properties, we have prepared two sets of biaxially oriented films using sequential and simultaneous stretching processes. Various properties manifested by these films were investigated<sup>1-3</sup> and the results related to the in-plane crystalline orientation distribution on the film properties are summarized below.

Figure 1 shows the changes in film dimensions as a function of TD draw ratios along the MD and TD measured by TMA at 50 and 105°C for sequentially and simultaneously stretched films. The expansion of the films at 50°C along the MD reduces continuously with increasing TD draw ratio while it slightly increases along the TD. There is a "crossover" point at the TD draw ratio of about 2.3×. At a "crossover" or "balance" point, the properties along the MD and TD become equal. A "crossover" point in the dimensional changes measured at 105°C is also observed at a similar TD draw ratio. However, dimensional changes at this temperature above the crossover point change from expansion to shrinkage. (A negative value indicates shrinkage, whereas positive values indicate expansion.) The absolute value of expansion or shrinkage will, therefore, be determined from the temperature and time of annealing of the films. In the present study, all the films were annealed at 200°C for 5 min. In simultaneously stretched films, MD and TD dimensional changes become equal at equal draw ratios, i.e., 3.5 × 3.5.

Figure 2 shows the variation in tensile modulus, F-5 (stress at 5.0% strain), tensile strength, and percent elongation at break along the MD and TD with the TD draw ratio for sequentially stretched film. The extent of anisotropy in the mechanical property is larger in the first stretching direction (MD) than in the transverse direction (TD) for TD draws below the balance point; the sense of the anisotropy is reversed after the balance point. At equal draw ratios, all properties are dominant in the TD direction. It is important to note that crossover points in various mechanical properties are observed at different TD draw ratios. For example, the crossover point in tensile modulus occurs at a TD draw ratio of 2.7×, whereas in tensile strength and percent elongation at break, it occurs at a TD draw ratio of 3.0×. In simultaneously stretched films, all the above-mentioned mechanical properties become equal at equal draw ratios (3.5 × 3.5). These results

lead to the conclusion that sequentially and simultaneously stretching processes promote different molecular deformation mechanisms.

As seen from Figure 3, the percent crystallinity of all sequentially and simultaneously stretched annealed films remains almost the same. Therefore, any change in film properties discussed so far in the annealed films is not due to a change in crystallinity of the film.

A question arises as to why sequentially stretched films show different crossover points at different TD draw ratios for various film properties, and why in simultaneously stretched films all MD and TD properties remain equal at equal draw ratios. To answer the above question, we have tried to understand the variation in film properties in terms of the crystalline, amorphous, and overall molecular orientation in the film plane.

Orientation distribution of crystals in the plane of the film can be derived from the *c*-axis orientation within the crystals using the pole figure analysis. Detailed information regarding the pole figure analysis has been discussed previously.<sup>3</sup>

The first column of Figure 4 shows ( $\bar{1}05$ ) pole figures for sequentially stretched PET films for various TD draw ratios. It can be seen that in uniaxially stretched films the crystals with the *c*-axis are oriented along the MD. Increasing the TD drawing leads to transformation of the MD oriented crystallites toward TD. At a TD draw ratio of 2.25×, a dual crystal orientation develops, whereas at an equal draw ratio (3.5 × 3.5), the *c*-axis of the crystals is oriented toward the TD. A balance point for crystal orientation occurs at a TD draw ratio of about 2.3×. Such a situation was not observed in the simultaneously stretched films; instead, the MD-oriented crystallites smoothly transform in the film plane and achieve an in-plane isotropic distribution at equal draw ratios.

The above results can also be confirmed from WAXS and electron micrographs shown, respectively, in the second and third columns of Figure 4. WAXS from uniaxially stretched films shows a fiber pattern, i.e., a uniaxial, cylindrically symmetric pattern. All the reflections from (*hk*0) are on the equator. They were indexed previously.<sup>2</sup> The unit cell of the PET crystals is triclinic; the (100) and (010) planes are parallel to the *c*-axis, whereas ( $\bar{1}05$ ) is almost perpendicular to the chain axis. These reflections, therefore, become a useful basis for monitoring changes taking place in the crystal orientation with TD draw ratios. Defocused electron micrographs of uniaxially oriented films show bright and dark contrast, representing, respectively, the amorphous and crystalline phases. It shows the la-

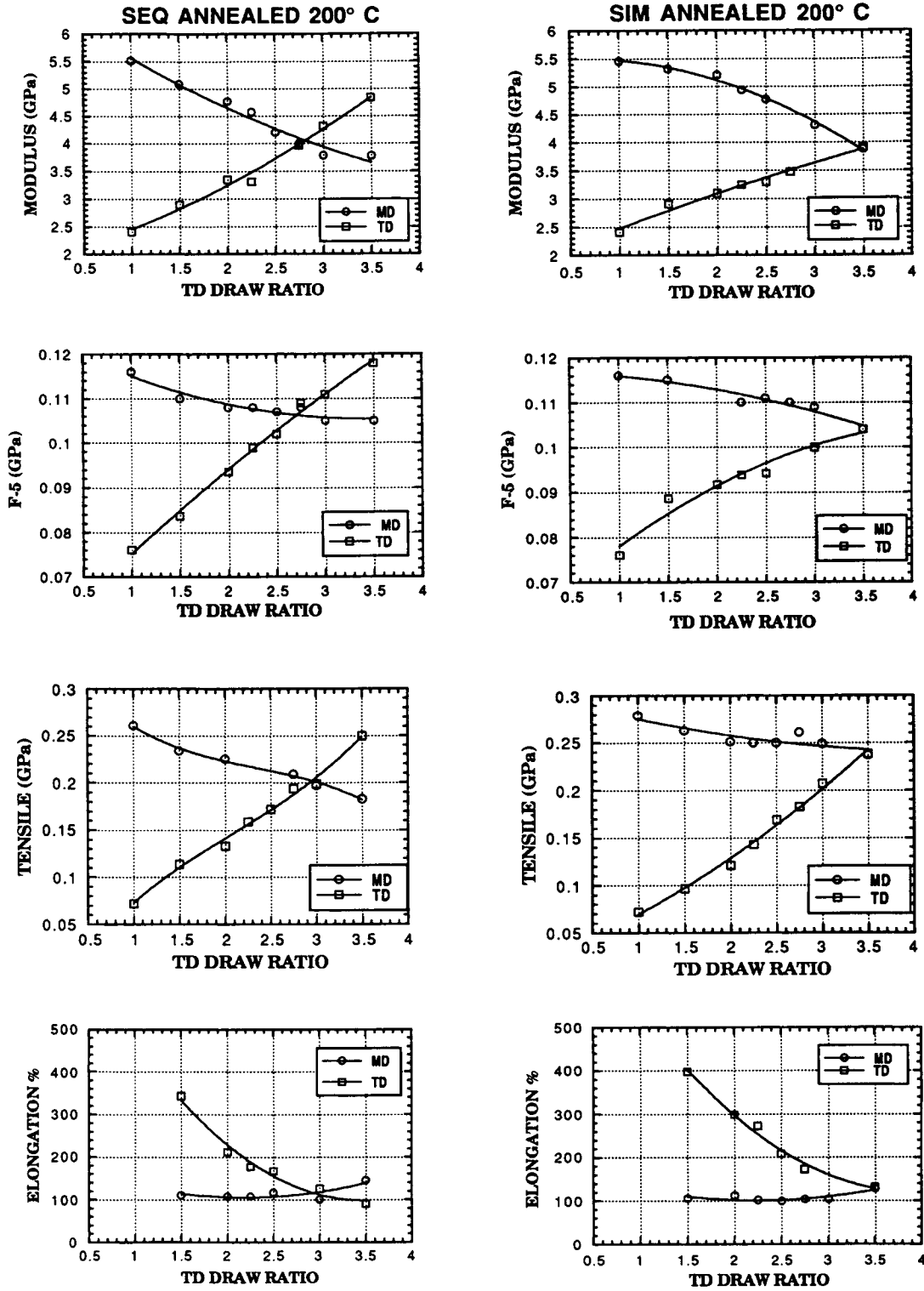


**Figure 2** Variation in tensile modulus, tensile strength, and elongation at break as functions of TD draw ratio for the film drawn by sequential and simultaneous biaxial stretching processes.

mellar nature of the crystals and their orientation in the film plane. From electron diffraction it is revealed that the *c*-axis in these crystals is along the

MD. The small-angle X-ray scattering (SAXS) pattern presented along with the electron micrograph in Figure 4 shows the presence of crystalline-

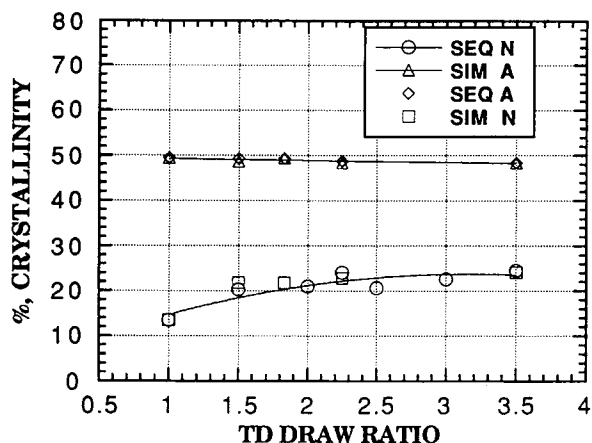


**Figure 3** Variation of percent crystallinity as a function of TD draw ratios for nonannealed and annealed (200°C) films.

amorphous periodicity along the MD. It shows that during MD stretching, MD-oriented crystalline network structure develops. In such a structure, lamellar<sup>13</sup> or needlelike crystals<sup>14,15</sup> are embedded in the amorphous matrix. In other words, crystallites in the amorphous phase act as physical tie points.

After stretching 3.5× along the MD, the strain-induced crystallized film samples were gradually stretched along the TD. At a TDX = 1.5, the equatorial reflections in the WAXS are broadened. However, the fiber pattern is not altered. Electron micrographs show that the orientation of lamellar crystals at this deformation (1.5×) is similar to that observed in uniaxially stretched film. The crystalline-amorphous periodicity is also predominantly along the MD. TD deformation up to 2.25× induces orientation of crystallites along both the MD and TD. One family of crystallites is oriented with chain axes along the MD; another set of the same family aligned along the TD. These results confirm the results of X-ray pole figures. At this stage, lamellar crystals, as seen from electron micrograph, evolved into equiaxial crystalline blocks. At equal draw ratios, WAXS shows that the *c*-axis of the crystals is overoriented along the TD; this fact is also noted in the X-ray pole figure. Electron micrographs show lamellar orientation similar to uniaxially oriented film, but in this case, the crystalline-amorphous periodicity is along the TD. In brief, (1) the crossover point in the crystal orientation occurs at a TD draw ratio of ca. 2.3× and (2) the results from wide- and small-angle X-ray pole figures and defocus electron microscopy are consistent.

Figure 5 shows the ( $\bar{1}05$ ) X-ray pole figures, WAXS, and SAXS for simultaneously stretched

films. The *c*-axis orientation within the crystallites, as evident from the ( $\bar{1}05$ ) pole figures and WAXS show a smooth and continuous transition from uniaxial to a planar random orientation. At the draw ratio of 3.5 × 3.5, isotropic in-plane crystalline orientation can be achieved. The SAXS pattern for uniaxially oriented film indicates a crystalline-amorphous periodicity, i.e., long spacing along the MD. It broadens out with increasing TD draw ratio and becomes isotropic at an equal draw ratio. At equal draw ratio, orientations of crystallites as well as long spacings become isotropic in the film plane.

Information regarding overall molecular orientations can be obtained from refractive index (RI) measurements. Figure 6 shows the variation in RI along the MD and TD for sequentially and simultaneously stretched films. With increasing TD draw ratios, RI increases along the TD while it decreases along the MD. In sequentially stretched films, a crossover point is noted at a TD draw ratio of 2.7×, whereas refractive indices become equal in simultaneously stretched films at equal draw ratios (3.5 × 3.5).

Information regarding the orientation of the amorphous phase along the MD and TD was derived from polarized fluorescence spectroscopy. The "orientation ratio," which is a measure of orientation of the amorphous phase along the MD and TD for sequentially and simultaneously stretched films, is shown in Figure 7. In sequentially stretched films, the orientation of the amorphous molecules remained almost constant up to a TD draw of 2.0×; a cause of this behavior in annealed films was discussed previously.<sup>1</sup> Thereafter, amorphous orientation decreases along the MD and increases along the TD; a crossover point is noted at the TD draw ratio of 3.0×. In simultaneously stretched films, the orientation of the amorphous phase decreases and increases, respectively, along the MD and TD and becomes equal at equal draw ratios.

All the above results concerning the variation in different orientations as well as properties for sequentially and simultaneously stretched films are schematically depicted in Figure 8. The crossover points corresponding to crystalline, overall molecular, and amorphous molecular orientation occur, respectively, at the TD draw ratios of 2.3×, 2.7×, and 3.0×. In simultaneously stretched film, all the orientation becomes equal at equal draw ratio, i.e., 3.5 × 3.5.

From a comparison of various orientations and properties, it can be concluded that when crystal orientation becomes equal along the MD and TD, the shrinkage at 105°C or expansion at 75°C be-

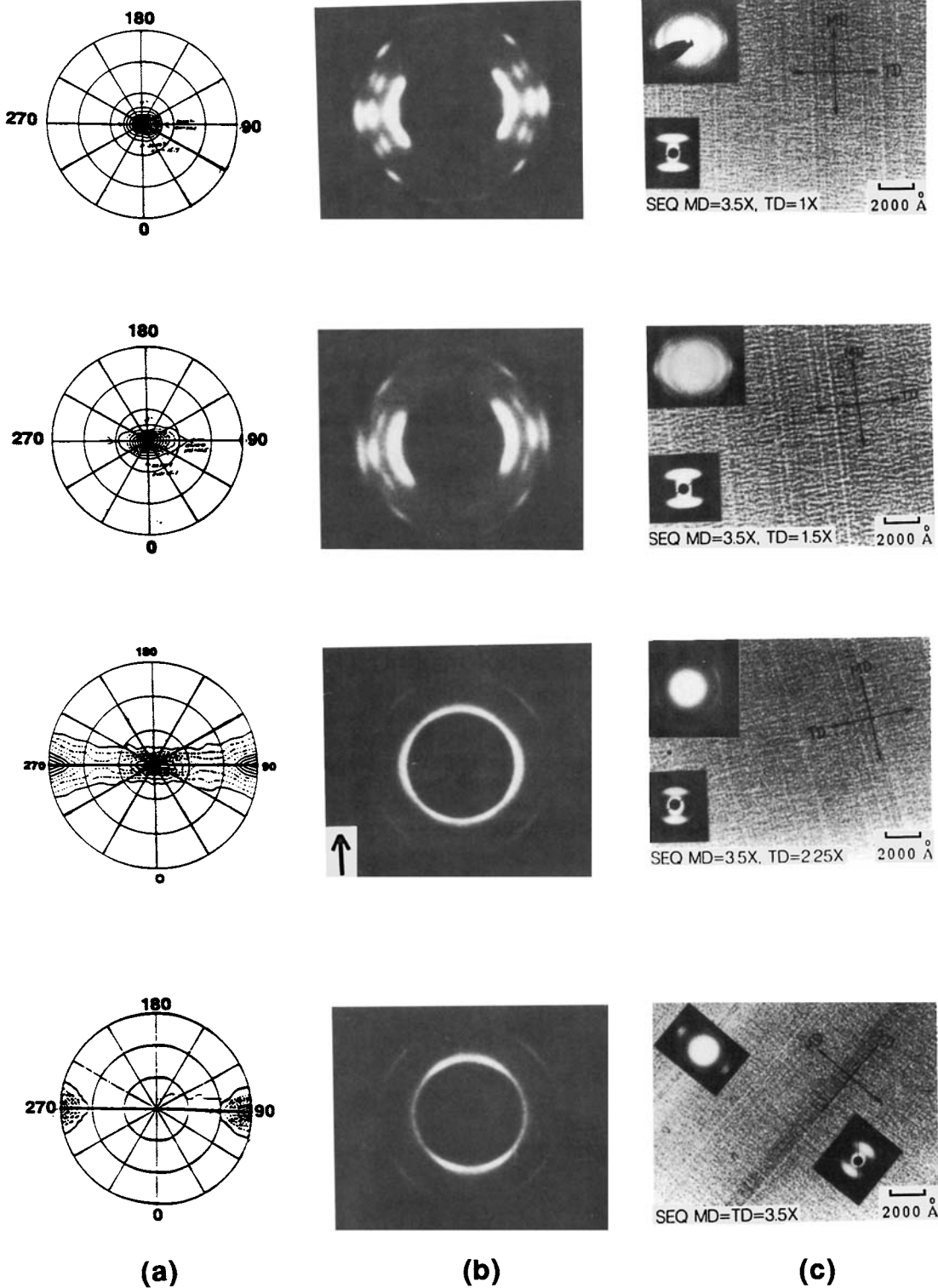
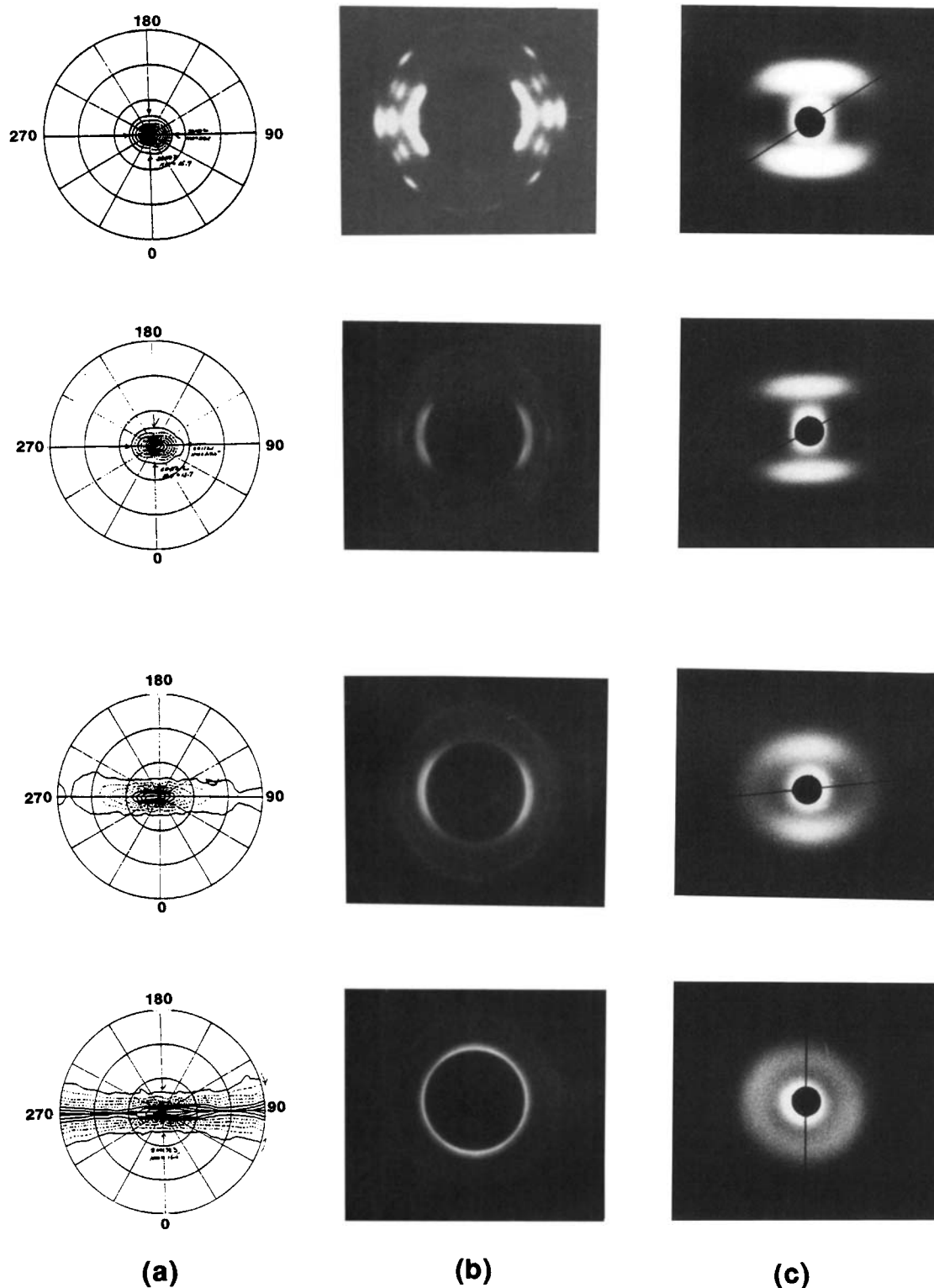


Figure 4 ( $\bar{1}05$ ) X-ray pole figures, WAXS, and electron micrographs for sequentially biaxially oriented PET films. Arrow indicates MD or *c*-axis direction. In the pole figure, the MD is perpendicular to the plane of the page (see also Ref. 2).



**Figure 5**  $(\bar{1}05)$  X-ray pole figures, WAXS, and SAXS for simultaneously stretched film at different TD stretch ratios.

comes equal. When overall molecular orientation becomes equal along the MD and TD, the tensile modulus and value of F-5 become equal, and when

orientation of the amorphous phase becomes equal along the MD and TD, tensile strength and % elongation at break become equal. In simultaneously



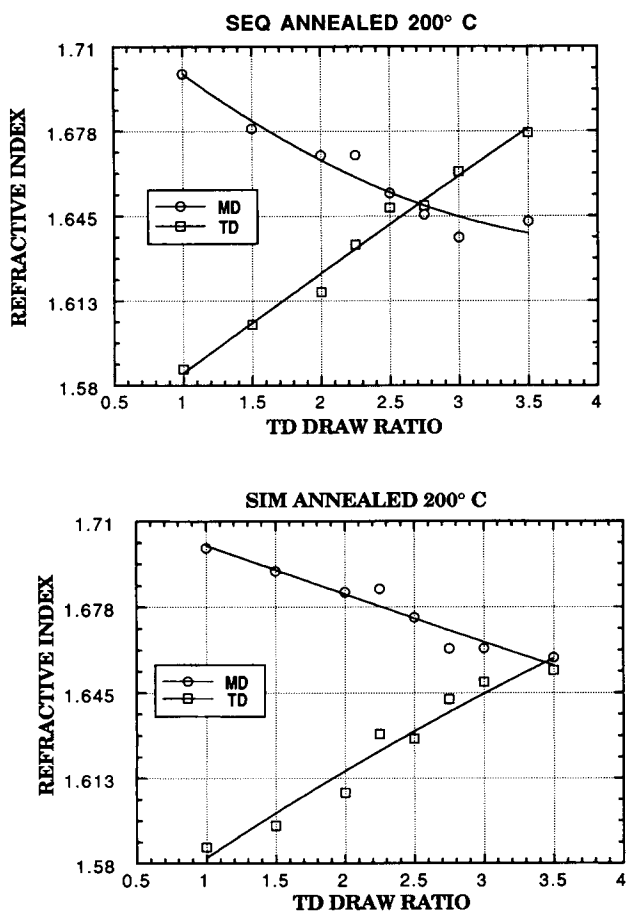


**Figure 6** Variation of refractive index along the MD and TD as a function of TD stretch ratio for sequentially and simultaneously stretched films.

stretched films, all orientations become equal along the MD and TD at equal draw ratios ( $3.5 \times 3.5$ ); therefore, all the film properties become equal at an equal draw ratio. It is apparent that dependency of film properties on the various types of orientations cannot be evaluated from the films prepared by simultaneous biaxial stretching process.

The above conclusions can be further extended for in-plane properties of the films. A film having in-plane isotropic expansion at  $75^\circ\text{C}$  or shrinkage at  $105^\circ\text{C}$  can be prepared by inducing in-plane isotropic crystalline orientation. Similarly, a film having isotropic tensile modulus and tensile strength can be prepared, respectively, by achieving in-plane isotropic overall molecular and amorphous orientation. The above facts can be strengthened by comparing in-plane distributions of the expansion and amorphous phases.

Variation in the in-plane distribution of the amorphous phase as a function of the TD draw ratio for annealed and nonannealed films was discussed

previously.<sup>1</sup> Results for annealed films prepared by sequential and simultaneous stretching process are shown in Figure 9. The in-plane variation of percent expansion at  $75^\circ\text{C}$  for sequentially and simultaneously oriented films is shown in Figure 10. A comparison of in-plane amorphous orientation and film expansion manifests a reversed correlation between these properties. For example, in uniaxially oriented films, the amorphous phase is more oriented toward the MD; however, the expansion measured at 50 and  $75^\circ\text{C}$  is lower along the MD. Note that in uniaxially oriented films crystals are oriented along the MD, so crystallites that act as physical tie points exert greater constraints on the MD-oriented molecules. This will restrict the shrinkage of the oriented molecules.

A situation in biaxially oriented film can be envisaged from comparison of the polar plots shown in Figures 9 and 10. Polar plots of the distribution of the amorphous phase<sup>1</sup> manifest that TD stretching of MD stretched films transform the MD-oriented amorphous phase toward the TD. Up to TD

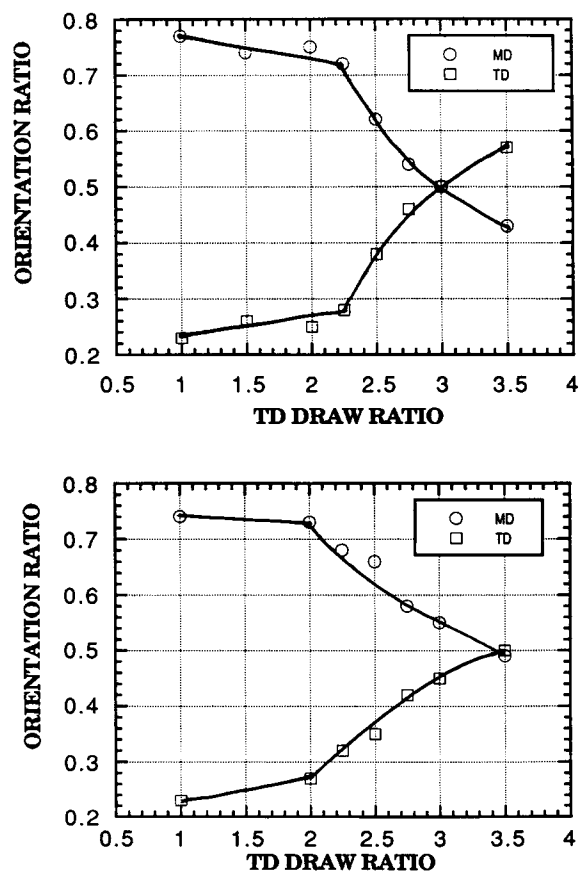


**Figure 7** Variation in the "amorphous orientation ratio" (AOR) along the MD and TD for sequentially (top figure) and simultaneously biaxially stretched films.

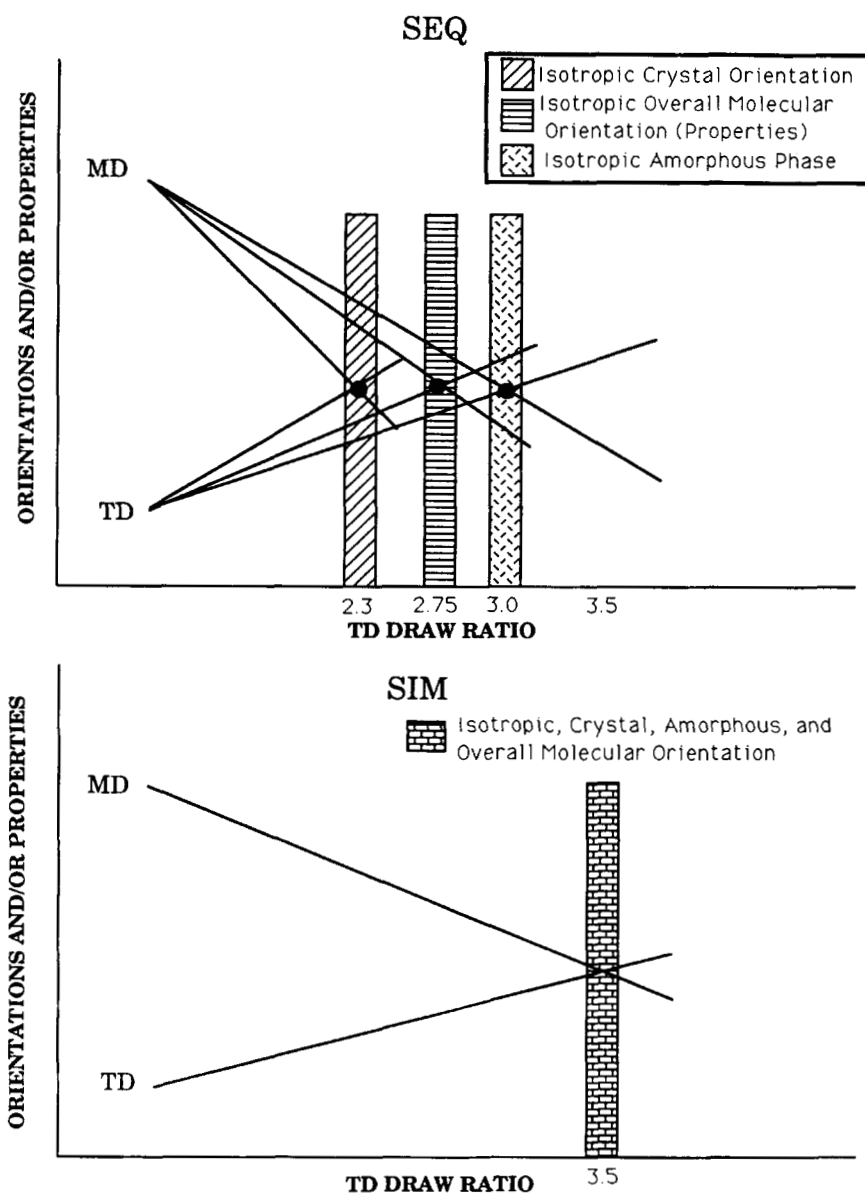


**Figure 8** Schematic representation manifesting the locations of crossover points noted in various orientations and properties at different TD draw ratios during the sequential stretching process. Note that all the in-plane orientations and properties become isotropic at equal draw ratios ( $3.5 \times 3.5$ ) in simultaneously stretched films (bottom figure).

draw ratios of about  $2.5\times$ , the in-plane distribution of the amorphous phase along the MD and TD is anisotropic. However, below this ratio, the in-plane expansion at  $75^\circ\text{C}$  and the orientation of crystallites are almost isotropic. This is a further indication that distribution of crystallites plays an important role. Moreover, the distribution of amorphous phase becomes almost isotropic at a TD draw ratio of  $3.0\times$ , but in-plane variation in the values of film expansion as well as orientation distribution of crystallites are anisotropic. At equal draw ratios of  $3.5 \times 3.5$ , the

orientation of the crystals and the amorphous phase is principally along the TD, but the expansion is greater along the MD. In general, the expansion of the oriented film at  $75^\circ\text{C}$  is lower in the direction of *c*-axis orientation within the crystals; thus the directionality of orientation of crystallites plays an important role in controlling film properties.

In the case of simultaneously stretched films, the dumbbell-shaped distribution of expansion at  $75^\circ\text{C}$  converts to hexagonal and then assumes a circular shape as stretching proceeds. Such isotropic distri-

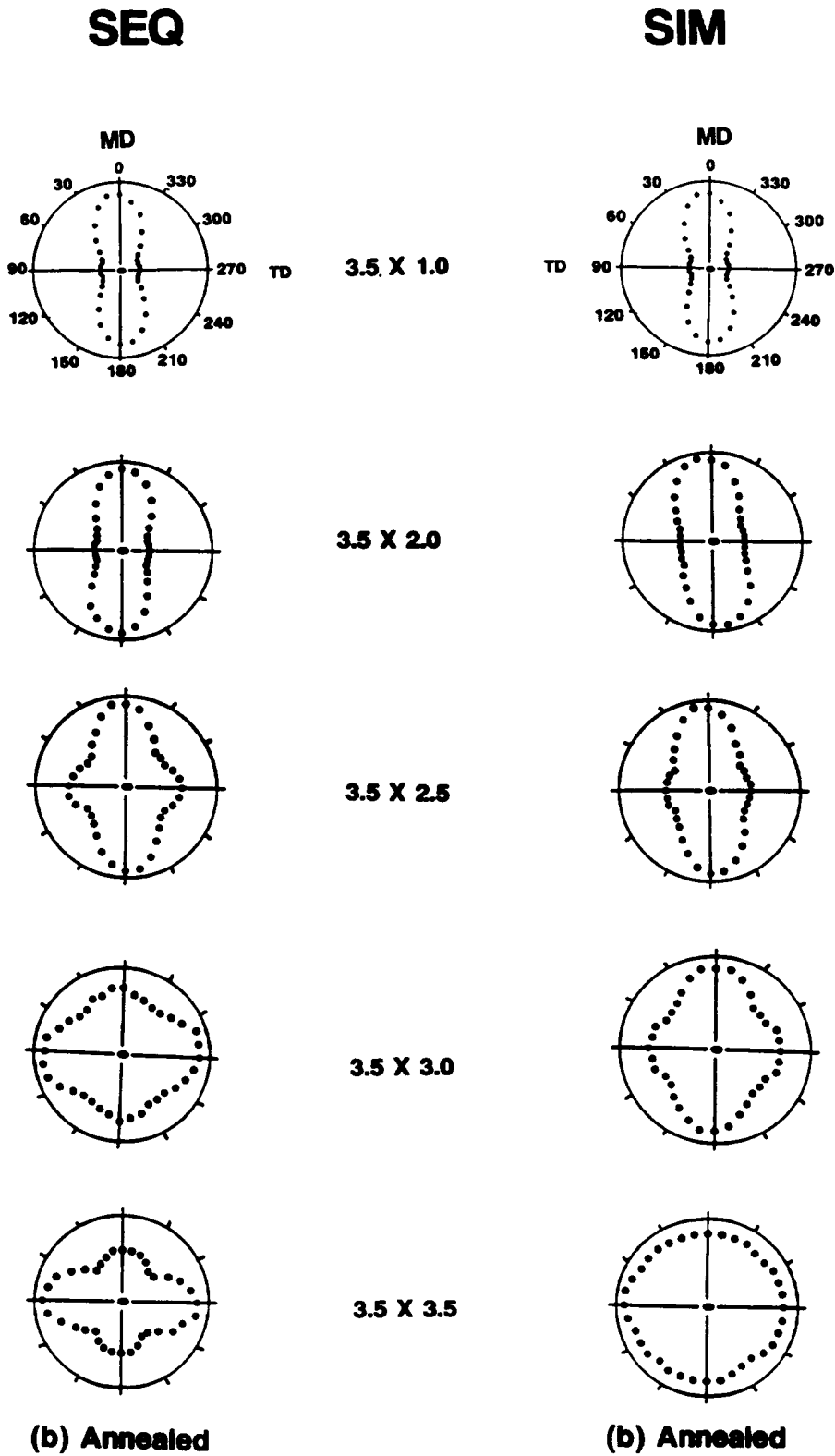


**Figure 9** The effect of TD draw ratio on the in-plane distribution of the amorphous phase in the films prepared by sequential and simultaneous biaxial stretching processes. MD draw ratio for all the films is 3.5 $\times$ , whereas TD draw ratios are varied (see Ref. 1).

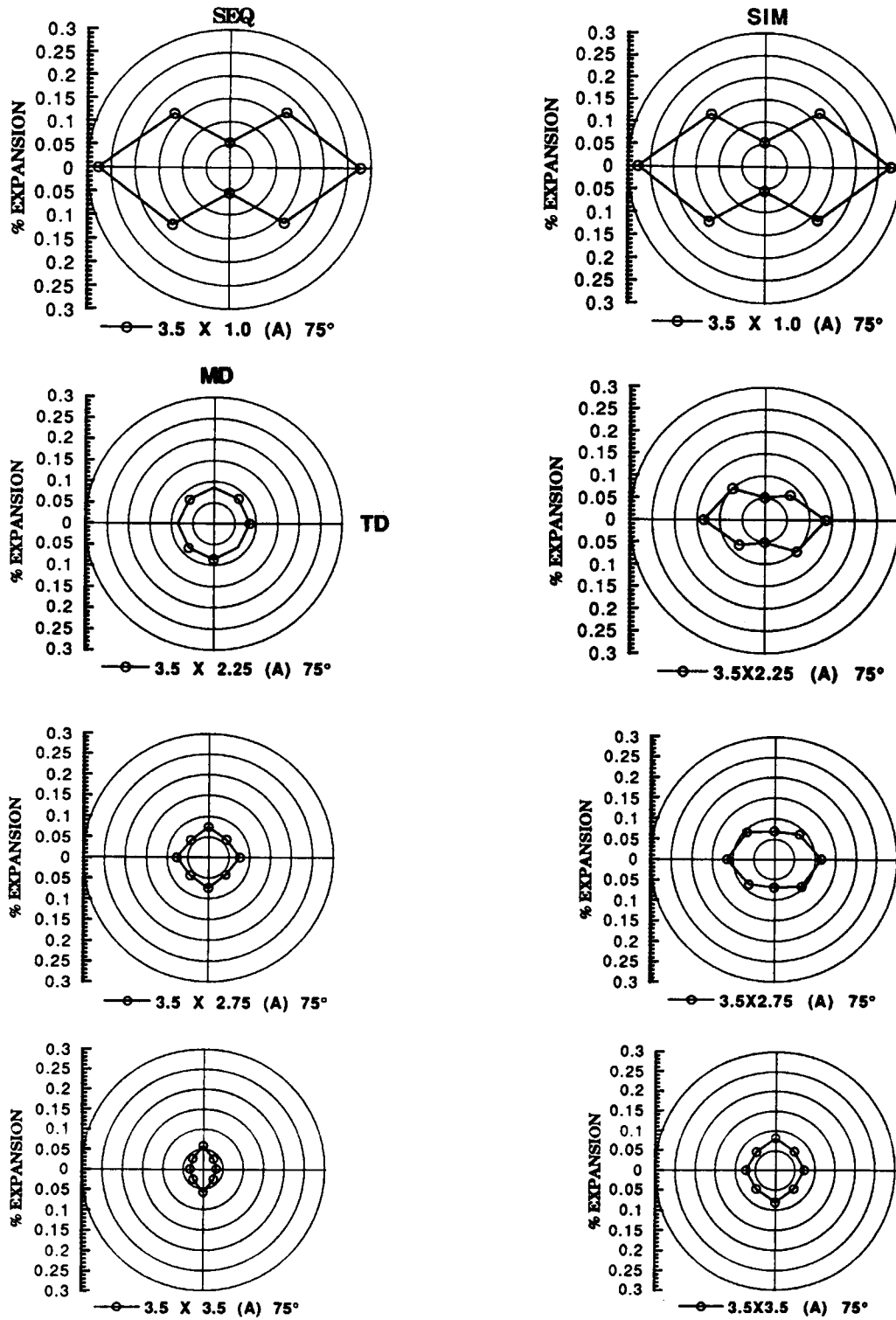


**Figure 10** The effect of TD draw ratios on the in-plane distribution of expansion of films at 75°C for sequentially and simultaneously stretched films.

bution of the amorphous phase is not achieved in sequentially stretched films at a TD draw ratio of 3.0 $\times$ . At equal draw ratios, the *c*-axis orientation (Fig. 1) as well as overall molecular orientation also becomes isotropic. From the sequentially stretched films, it is apparent that the crystalline orientation is responsible for isotropic expansion of the film. From the polar plots it is evident that, in general, biaxial stretching improves the in-plane dimensional stability of the films. The magnitude of expansion or shrinkage depends on the degree of crystallinity as well as molecular orientation, annealing temperature, and time. It indicates that orientation of the amorphous molecules, the crystal orientation, and nature of constraint imposed on the amorphous molecules by the crystallites play an important role in achieving in-plane isotropy in this property. The above mechanism directs one in preparing a film having an in-plane isotropic expansion or shrinkage with its desired magnitude.

From these results, it can be concluded that orientation of amorphous molecules in semicrystalline polymers alone do not provide criteria to define the properties like expansion or shrinkage; the constraint on the molecules determines the final values of such properties. In the crystalline network structure of PET for a particular molecular weight, constraints on the molecules are determined by several factors like orientation of molecules, percent crystallinity, volume fraction of interconnecting tie molecules, and constraint imposed on these molecules due to the proximity of the crystallites, etc. In a highly oriented system, a highly constrained amorphous phase develops in the condition when the films are heat-treated sufficiently in the temperature range where the rate of crystallization is maximum and molecular relaxation rate assumes a minimum value. Usually due to strain-induced crystallization, constraints on the molecules are greater in the direction where molecular orientation is maximum. In this direction, the expansion will be lower. A detailed study on the nature of the constraint on the molecules at different orientations of the molecules in the PET films and heat treatment has been discussed previously.<sup>3</sup>

It is also evident that certain mechanical properties are not greatly influenced by the crystalline phase. In the present system, tensile strength and elongation at break are found to depend mainly on orientation of the amorphous phase; crystal orientation has no appreciable influence. However, for greater generalization, the role of size, perfection, and volume fraction of crystallites on such properties need to be investigated.

The crossover points noted in various orientation and properties in sequentially stretched films are found to be a function of processing parameters and a study along this direction will be published separately.<sup>16</sup>

## CONCLUSIONS

For achieving isotropic in-plane expansion in biaxially oriented films, it is necessary to achieve isotropic in-plane crystal orientation. In semicrystalline polymers, the final values of film expansion or shrinkage are determined from the constraints imposed on the molecules and not from the molecular orientation alone. Obtaining in-plane isotropic tensile strength and elongation at break is found to be entirely dependent on achieving an isotropic distribution of the amorphous orientation; the orientation of crystallites plays no detectable role.

Sequential and simultaneous stretching processes follow different deformation mechanisms. During sequential stretching of films at a temperature and strain rate, the MD-oriented crystalline and amorphous phase changes to an intermediate state with random orientation within the film plane. At equal draw ratios, both orientation and film properties are predominantly along the TD. In this stretching process, the balance points for different orientation (crystalline, amorphous, and overall molecular orientation) occur at different TD draw ratios. Therefore, it is difficult to balance all the properties of the film by the sequential stretching process. In simultaneously biaxially stretched films, the orientation remains isotropic at equal draw ratios; therefore, all the properties also remain isotropic at equal draw ratios. Thus, the simultaneous stretching method can be considered as an excellent balanced film-fabricating process.

The author is thankful to Frank Wilson, David Salem, Hao Chang, John Cooper, and Mel Simpson for their help in the experimental work. Special thanks to Drs. Ross Lee and John Barkley for the inspiration for this work.

## REFERENCES

1. R. M. Gohil and D. Salem, *J. Appl. Polym. Sci.*, **47**, 1989 (1993).
2. H. Chang, J. M. Schultz, and R. M. Gohil, *J. Macromol. Sci. Phys.* **B32**, 99 (1993).
3. R. M. Gohil, *J. Appl. Polym. Sci.*, **48**, 1649 (1993).

4. R. M. Gohil, *Proc. 49th Ann. Mtg. EMSA*, 1056 (1991).
5. K. Matsumoto, H. Ieki, and R. Imamura, *J. Fiber Sci. (Sen I Gakkaishi)*, **27**(12), 516 (1971); **28**(6), 189 (1972).
6. K. Matsumoto, Y. Izumi, and R. Imamura, *J. Fiber Sci.*, **29**(9), 53 (1973).
7. C. J. Heffelfinger and P. G. Schmidt, *J. Appl. Polym. Sci.*, **9**, 2661 (1965).
8. C. J. Heffelfinger and R. L. Burton, *J. Polym. Sci.*, **47**, 289 (1960).
9. J. L. Koenig and S. W. Cornell, *J. Macromol Sci. (Phys.) B*, **1**(2), 279 (1967).
10. S. A. Jabarin, *Polym. Eng. Sci.*, **24**(5), 379 (1984).
11. E. W. Fischer and S. Fakirov, *J. Mat. Sci.*, **11**, 1041 (1976).
12. R. J. Samuels, *Structured Polymer Properties* Wiley, New York, 1974.
13. R. M. Gohil and J. Petermann, *J. Polym. Sci. Polym. Phys. Ed.*, **17**, 525 (1979).
14. R. M. Gohil and J. Petermann, *J. Mat. Sci.*, **18**, 1719 (1983).
15. J. Petermann, R. M. Gohil, and M. Massud, *J. Mat. Sci.*, **17**, 100 (1982).
16. R. M. Gohil, unpublished work.

Received June 25, 1992

Accepted July 22, 1992